

Exploration of CPT violation via time-dependent geometric quantities embedded in neutrino oscillation through fluctuating matter

Zisheng Wang^{1,2,*} and Hui Pan^{2,†}

¹*College of Physics and Communication Electronics,
Jiangxi Normal University, Nanchang 330022, P. R. China*

²*Institute of Applied Physics and Materials Engineering,
Faculty of Science and Technology, University of Macau, Macao SAR, China*

We propose a new approach to explore CPT violation of neutrino oscillations through a fluctuating matter based on time-dependent geometric quantities. By mapping the neutrino oscillations onto a Poincaré sphere structure, we obtain an analytic solution of master equation and further define the geometric quantities, i.e., radius of Poincaré sphere and geometric phase. We find that the mixing process between electron and muon neutrinos can be described by the radius of Poincaré sphere that depends on the intrinsic CP-violating angle. Such a radius reveals a dynamic mechanism of CPT-violation, i.e., both spontaneous symmetry breaking and Majorana-Dirac neutrino confusion. We show that the time-dependent geometric phase can be used to find the neutrino nature and observe the CPT-violation because it is strongly enhanced under the neutrino propagation. We further show that the time-dependent geometric phase can be easily detected by simulating the neutrino oscillation based on fluctuating magnetic fields in nuclear magnetic resonance, which makes the experimental observation of CPT-violation possible in the neutrino mixing and oscillations.

PACS numbers: 14.60.Pq, 03.65.Vf, 03.65.Yz

I. INTRODUCE

Neutrino mixing and oscillations are important to investigate new physics beyond the Standard Model of elementary particle physics, and also involve in hot issues on both astro-particle physics and cosmology [1–3]. Experimentally and theoretically, a set of important and fundamental problems, such as the neutrino mass, the nature of the Dirac vs Majorana neutrino or Majorana-Dirac confusion theorem [4], and the validity of CPT symmetry, has been under the debate [5–9]. The interference of the neutrino oscillations [10, 11] can be used to test the CPT symmetry and the neutrino nature based effectively on the geometric phase, which provides an unconventional approach to probe CPT-violation beside the neutron electric dipole moment [12].

The evolution of neutrinos involved the weak interactions leads to the CP-violation in a given flavor space, where the extrinsic CP-violating phases can mimic the characteristics of intrinsic CP-violating phases in the leptonic mixing matrix [13, 13–16].

The neutrino oscillations observed so far can be explained in terms of three flavor space, i.e., active electron neutrino ν_e , muon neutrino ν_μ and τ neutrino ν_τ , where the extrinsic CP violation is disentangled from the intrinsic one by the CP-violating observable [17]. An alternative method to treat neutrino oscillations has attracted extensive interests

*zishengwang@yahoo.com

†huiipan@umac.mo

in terms of analogizing with simple and intuitive Rabi-oscillations in a two-flavor space [1, 18], where the extrinsic CP-violating phases can exactly appear in the two-level Hamiltonian.

In principle, such a CP-violating phase can be observed in neutrinoless double beta decay (NDBD) in terms of the transition probability, but it is an extremely low efficiency of direct neutrino measurements so as to have not fully solve this problem in the experiments up to now.

The characteristics of mixed neutrino evolution can be recognized by the geometric phase [19, 20]. Especially, such a geometric phase can be observed in the experiments. In the neutrino mixing and oscillations, the neutrino system interacts irreversibly with its surrounding environment [21, 22], resulting in statistical mixtures of quantum superpositions. To date, most studies of geometric phase have been focused on the pure state by using quantum mechanics in terms of a closed system [11] or have not included the two-state mixing effects in the open system [20, 23, 24], which are unsuitable for neutrino mixing and oscillations. It is, therefore, necessary to find out the mechanism of flavor neutrino mixing and oscillations in the geometric phase just like the mixed state of open system.

In this work, we map the two-flavor neutrino oscillations onto a three-dimensional Poincaré sphere structure. We find that the time-dependent radius of Poincaré sphere can describe neutrino mixture degree of freedom and reveal a dynamic mechanism of CPT violation. We further investigate the relations between the time-dependent geometric quantities and CPT violation. Finally, we propose a new approach to detect the geometric phase with the CPT-violating effects by quantum simulation of physical fluctuating fields.

II. HAMILTONIAN WITH A CP-VIOLATING PHASE

Let us consider solar neutrinos with small square-mass difference $\Delta m_{21}^2 = m_2^2 - m_1^2$ between the neutrinos ν_μ and ν_e , where the large squared-mass ones Δm_{31}^2 and Δm_{32}^2 between ν_τ and ν_e and between ν_τ and ν_μ are averaged out [1, 2]. Under the mass scale dominant approximation and in the ultra-relativistic limit $p \approx E$, the Hamiltonian \mathcal{H} with an intrinsic CP-violating phase ϕ for two flavor neutrino oscillations in medium can be expressed as [1, 5]

$$\mathcal{H} = \left(E + \frac{m_1^2 + m_2^2}{4E} + \frac{V_0}{2} \right) \mathcal{I}_{2 \times 2} + \frac{1}{2} \begin{pmatrix} V_0 - \frac{\Delta m_{21}^2}{2E} \cos 2\theta & \frac{\Delta m_{21}^2}{2E} e^{-i\phi} \sin 2\theta \\ \frac{\Delta m_{21}^2}{2E} e^{i\phi} \sin 2\theta & -V_0 + \frac{\Delta m_{21}^2}{2E} \cos 2\theta \end{pmatrix}, \quad (1)$$

where θ is a neutrino mixing angle in vacuum and $V_0 = \sqrt{2}G_F n_e \cos^2 \theta_{13}$ is a matter potential with the Fermi weak coupling constant G_F , the electron density n_e in the medium, and the oscillation parameter $0.953 < \cos^2 \theta_{13} \leq 1$ under 3σ bound. In terms of Mikheyev-Smirnov-Wolfenstein effect, the CP asymmetric matter potential V_0 can enhance and suppress the oscillations in the neutrino and antineutrino channels, respectively.

Since $\mathcal{I}_{2 \times 2}$ is a 2×2 identity matrix, the first term with non-zero trace on the right of Eq. (1) adds only an unimportant overall phase factor to the time-evolving state in the neutrino mixing and oscillations. The second term

can be divided into diagonal and nondiagonal parts, which can be expanded in terms of Pauli matrices (i.e., σ_z, σ_x and σ_y). Since only σ_y changes sign under the charge conjugation and parity (CP) transformation, ϕ is an intrinsic CP-violating (or Majorana) phase. For the Dirac neutrino, ϕ can be eliminated by a $U(1)$ gauge transformation. In contrast, the rephasing of the left-chiral massive neutrino field is not possible for the Majorana neutrino because the mass term of the Lagrangian is not invariant under the gauge transformation.

In the Schrödinger picture, the amplitude $\Psi_{\alpha\beta}(t) = \langle \nu_\beta(0) | \nu_\alpha(t) \rangle$ of neutrino transition $\nu_\alpha \rightarrow \nu_\beta$ ($\alpha = e, \nu = e, \mu$) is evolved by [1]

$$i \frac{d}{dt} \Psi_{\alpha\beta}(t) = \mathcal{H} \Psi_{\alpha\beta}(t), \quad (2)$$

in the units $\hbar = 1$, where the overall phase factor from the first term of Hamiltonian \mathcal{H} (See Eq. (1)) can be eliminated by the phase shift,

$$\Psi_{\alpha\beta}(t) = \psi_{\alpha\beta}(t) \exp \left(-i \left(E + \frac{m_1^2 + m_2^2}{4E} + \frac{V_0}{2} \right) t \right). \quad (3)$$

Thus the relevant evolution equation can be expressed in terms of the matrix form, i.e.,

$$i \frac{d}{dt} \begin{pmatrix} \psi_{ee}(t) \\ \psi_{e\mu}(t) \end{pmatrix} = \frac{1}{4E} \begin{pmatrix} -\Delta m_{21}^2 \cos 2\theta + A_{cc} & \Delta m_{21}^2 \sin 2\theta e^{-i\phi} \\ \Delta m_{21}^2 \sin 2\theta e^{i\phi} & \Delta m_{21}^2 \cos 2\theta - A_{cc} \end{pmatrix} \begin{pmatrix} \psi_{ee}(t) \\ \psi_{e\mu}(t) \end{pmatrix}, \quad (4)$$

where $A_{cc} = 2EV_0$. In Eq. (4), $\psi_{ee}(t)$ and $\psi_{e\mu}(t)$ are the transitive amplitudes of $\nu_e \rightarrow \nu_e$ and $\nu_e \rightarrow \nu_\mu$, respectively. The evolution equation (4) is a Schrödinger-like equation with effective Hamiltonian matrix in the flavor basis, which can be simplified by a unitary transformation,

$$\begin{pmatrix} \psi_{ee}(t) \\ \psi_{e\mu}(t) \end{pmatrix} = U_M \begin{pmatrix} \phi_{e1}(t) \\ \phi_{e2}(t) \end{pmatrix}, \quad (5)$$

and

$$\mathcal{H}_M = U_M^\dagger \frac{1}{4E} \begin{pmatrix} -\Delta m_{21}^2 \cos 2\theta + A_{cc} & \Delta m_{21}^2 \sin 2\theta e^{-i\phi} \\ \Delta m_{21}^2 \sin 2\theta e^{i\phi} & \Delta m_{21}^2 \cos 2\theta - A_{cc} \end{pmatrix} U_M = \frac{1}{4E} \begin{pmatrix} -\Delta m_M^2 & 0 \\ 0 & \Delta m_M^2 \end{pmatrix}, \quad (6)$$

where \mathcal{H}_M is called as an effective Hamiltonian matrix in matter in terms of the mass basis and the effective squared-mass difference in matter is given by

$$\Delta m_M^2 = \sqrt{(\Delta m_{21}^2 \cos 2\theta - A_{cc})^2 + (\Delta m_{21}^2 \sin 2\theta)^2}. \quad (7)$$

The unitary matrix in Eqs. (5) and (6) can be expressed as

$$U_M = \begin{pmatrix} \cos \vartheta_M & \sin \vartheta_M e^{-i\phi} \\ -\sin \vartheta_M e^{i\phi} & \cos \vartheta_M \end{pmatrix}, \quad (8)$$

which is an effective mixing matrix with the effective mixing angle ϑ_M and the CP-violating phase in matter. The mixing angle ϑ_M in matter is written as

$$\tan 2\vartheta_M = \frac{\tan 2\theta}{1 - \frac{A_{cc}}{\Delta m_{21}^2 \cos 2\theta}}, \quad (9)$$

where there is a resonance when $A_{cc} = \Delta m_{21}^2 \cos 2\theta$. At the resonance the effective mixing angle is $\vartheta = \pi/2$, i.e., the mixing is maximal, leading to the possibility of total transitions between the two flavors if the resonance region is wide enough.

Inserting Eqs. (5) and (6) into Eq. (4), one has

$$i \frac{d}{dt} \begin{pmatrix} \phi_{e1}(t) \\ \phi_{e2}(t) \end{pmatrix} = \frac{1}{4E} \begin{pmatrix} -\Delta m_M^2 & 0 \\ 0 & \Delta m_M^2 \end{pmatrix} \begin{pmatrix} \phi_{e1}(t) \\ \phi_{e2}(t) \end{pmatrix}, \quad (10)$$

with the initial conditions,

$$\begin{pmatrix} \phi_{e1}(0) \\ \phi_{e2}(0) \end{pmatrix} = U_M^\dagger \begin{pmatrix} \psi_{ee}(0) \\ \psi_{e\mu}(0) \end{pmatrix} = \begin{pmatrix} \cos \vartheta_M & -\sin \vartheta_M e^{-i\phi} \\ \sin \vartheta_M e^{i\phi} & \cos \vartheta_M \end{pmatrix} \begin{pmatrix} 1 \\ 0 \end{pmatrix} = \begin{pmatrix} \cos \vartheta_M \\ e^{i\phi} \sin \vartheta_M \end{pmatrix}. \quad (11)$$

Eq. (10) is a decoupled evolution of the amplitudes of effective massive neutrinos in matter. Under the initial condition (11), its solution is direct. We find

$$\begin{pmatrix} \phi_{e1}(t) \\ \phi_{e2}(t) \end{pmatrix} = \begin{pmatrix} e^{i\frac{\Delta m_M^2}{4E}t} \cos \vartheta_M \\ e^{i(\phi - \frac{\Delta m_M^2}{4E}t)} \sin \vartheta_M \end{pmatrix}, \quad (12)$$

and

$$\begin{pmatrix} \psi_{ee}(t) \\ \psi_{e\mu}(t) \end{pmatrix} = \begin{pmatrix} \cos^2 \vartheta_M e^{i\frac{\Delta m_M^2}{4E}t} + \sin^2 \vartheta_M e^{-i\frac{\Delta m_M^2}{4E}t} \\ \frac{1}{2} e^{i\phi} \sin 2\vartheta (e^{-i\frac{\Delta m_M^2}{4E}t} - e^{i\frac{\Delta m_M^2}{4E}t}) \end{pmatrix}, \quad (13)$$

which leads to the transition probabilities,

$$P_{\nu_e \rightarrow \nu_\mu}(t) = |\Psi_{e\mu}(t)|^2 = |\psi_{e\mu}(t)|^2 = \sin^2 2\vartheta_M \sin^2 \left(\frac{\Delta m_M^2 t}{4E} \right), P_{\nu_e \rightarrow \nu_e}(t) = 1 - P_{\nu_e \rightarrow \nu_\mu}(t), \quad (14)$$

which the CP-violating (or Majorana) phase ϕ vanishes in the transition probability with the same structure as the two-neutrino transition probability in vacuum. As pointed by Giunti [25], such a Majorana phase of the neutrino mixing matrix cannot have any effect in the neutrino oscillations in the conventional Hilbert space.

III. NEUTRINO MIXING AND OSCILLATIONS IN DISSIPATIVE MATTER

It is known that the CP-violating effects can not be described in the two-flavor neutrino mixed states in terms of the conventional Hilbert space. In reality, no quantum system is completely isolated from its surroundings, so the neutrino system is open to some extent, causing dissipation in the quantum system. When the neutrino propagates through a dissipative matter, the neutrino mixing and oscillations should be extended to an open quantum system including the interactions between the neutrino and its external environment.

In this situation, a density matrix $\rho(t)$ needs to be introduced in order to describe the two-flavor neutrino mixed states with the synthesized properties, i.e., hermitian, positive operators with non-negative eigenvalues, and unit trace. The dynamic evolution of neutrino mixing and oscillations can be described by the Lindblad master equation [26], i.e.,

$$\frac{d}{dt}\rho(t) = -i[\mathcal{H}, \rho(t)] + \mathcal{L}\rho, \quad (15)$$

in the units $\hbar = 1$, where the Lindblad superoperator is given by

$$\mathcal{L}\rho = \frac{1}{2} \sum_{i,j=x,y,z} c_{ij}([\sigma_i\rho, \sigma_j] + [\sigma_i, \rho\sigma_j]), \quad (16)$$

where the summation runs to $N^2 - 1 = 2^2 - 1$ for the two-dimensional quantum system and therefore includes all possible decay ways with the constant coefficients $c_{ij} \geq 0$ due to the interaction between the neutrinos and dissipative environment.

Differently from the Schrödinger picture in Eq. (2), the master equation (15) incorporates decoherent effects due to energy loss ($i \neq j$) or loss of pure phase information without energy ($i = j = z$). Thus Eq. (15) essentially goes beyond the standard Hamiltonian dynamics. The first term on the right of Eq. (15) is a usual Schrödinger term but includes the CP-violating effect as shown in Eq. (1). The second term leads to time-irreversibility. Therefore, we can explore the CPT violating effect in terms of the master equation (15).

At initial time ($t = 0$), the two flavor states, the electron neutrino $|\nu_e\rangle$ and the muon neutrino $|\nu_\mu\rangle$, are described by the pure states and can be represented by

$$|\nu_e(0)\rangle = \begin{pmatrix} \cos\theta \\ e^{i\phi}\sin\theta \end{pmatrix}, |\nu_\mu(0)\rangle = \begin{pmatrix} \sin\theta \\ -e^{i\phi}\cos\theta \end{pmatrix}, \quad (17)$$

with the corresponding density matrices,

$$\rho_e(0) = \begin{pmatrix} \cos^2\theta & \frac{1}{2}e^{-i\phi}\sin 2\theta \\ \frac{1}{2}e^{i\phi}\sin 2\theta & \sin^2\theta \end{pmatrix}, \rho_\mu(0) = \begin{pmatrix} \sin^2\theta & -\frac{1}{2}e^{-i\phi}\sin 2\theta \\ -\frac{1}{2}e^{i\phi}\sin 2\theta & \cos^2\theta \end{pmatrix}, \quad (18)$$

which can be reexpressed by the Pauli matrices, i.e., $\rho_e(0) = \frac{1}{2}(\mathcal{I}_{2\times 2} + \sin(2\theta)\cos\phi\sigma_x + \sin(2\theta)\sin\phi\sigma_y + \cos(2\theta)\sigma_z)$ and $\rho_\mu(0) = \frac{1}{2}(\mathcal{I}_{2\times 2} - \sin(2\theta)\cos\phi\sigma_x - \sin(2\theta)\sin\phi\sigma_y - \cos(2\theta)\sigma_z)$. Since the σ_y 's coefficients are not equal to zero, the initial density matrices carry with the CP-violating messages.

IV. POINCARÉ SPHERE STRUCTURE

A geometric representation of neutrino mixing and oscillations is an effective approach to understand and analyze the dynamic evolution of neutrino system [27, 28]. Therefore we map the neutrino oscillations in the dissipative matter

onto a Poincaré sphere by defining a Poincaré vector $\vec{n}(t) = \text{Tr}(\rho(t)\vec{\sigma})$, where the three components are given by

$$u(t) = \rho_{12}(t) + \rho_{21}(t), \quad (19)$$

which is a real part of the overlaps between the neutrinos ν_e and ν_μ , measuring a reflection between the two neutrinos,

$$v(t) = i(\rho_{12}(t) - \rho_{21}(t)), \quad (20)$$

which is an imaginary part of the overlaps, parameterizing an absorption between the two neutrinos, and

$$w(t) = \rho_{11}(t) - \rho_{22}(t), \quad (21)$$

which describes the transition $\nu_e \rightarrow \nu_\mu$ in process of the neutrino propagation.

The dynamics of neutrino oscillations described by the master equation is qualitatively converted into the Poincaré picture in terms of matrix form, i.e.,

$$\frac{d}{dt} \begin{pmatrix} u(t) \\ v(t) \\ w(t) \end{pmatrix} = \begin{pmatrix} -2\Gamma_{23} & -2\mathcal{B}_- & 2\mathcal{D}_+ \\ 2\mathcal{B}_+ & -2\Gamma_{13} & -2\mathcal{C}_- \\ -2\mathcal{D}_- & 2\mathcal{C}_+ & -2\Gamma_{12} \end{pmatrix} \begin{pmatrix} u(t) \\ v(t) \\ w(t) \end{pmatrix}, \quad (22)$$

where $\Gamma_{ij} = c_{ii} + c_{jj}$, $\mathcal{B}_+ = \frac{V_0}{2} \cos 2\theta - \frac{\Delta m_{21}^2}{4E} + c_{12}$, $\mathcal{B}_- = \frac{V_0}{2} \cos 2\theta - \frac{\Delta m_{21}^2}{4E} - c_{21}$, $\mathcal{C}_+ = \frac{V_0}{2} \sin 2\theta \cos \phi + c_{23}$, $\mathcal{C}_- = \frac{V_0}{2} \sin 2\theta \cos \phi - c_{32}$, $\mathcal{D}_+ = \frac{V_0}{2} \sin 2\theta \sin \phi + c_{31}$, and $\mathcal{D}_- = \frac{V_0}{2} \sin 2\theta \sin \phi - c_{13}$. Eq. (22) is called as a Poincaré equation of neutrino oscillations. In order to get its analytic solution [29], we firstly diagonalize the 3×3 matrix in Eq. (22).

The three diagonal elements are given by

$$\lambda_0 = -\frac{4}{3}\Gamma - \frac{2^{1/3}}{3} \frac{b}{(a + \sqrt{4b^3 + a^2})^{1/3}} + \frac{1}{3} \left(\frac{a + \sqrt{4b^3 + a^2}}{2} \right)^{1/3}, \quad (23)$$

and

$$\lambda_\pm = -\frac{4}{3}\Gamma + \frac{1 \pm i\sqrt{3}}{3} \frac{b}{[4(a + \sqrt{4b^3 + a^2})]^{1/3}} - \frac{1 \mp i\sqrt{3}}{6} \left(\frac{a + \sqrt{4b^3 + a^2}}{2} \right)^{1/3}, \quad (24)$$

with $a = 8(27\mathcal{B}_+\mathcal{C}_+\mathcal{D}_+ + 9\mathcal{C}_+\mathcal{C}_-(\Gamma_{12} + \Gamma_{13} - 2\Gamma_{23}) + (9\mathcal{D}_+\mathcal{D}_- - (\Gamma_{12} + \Gamma_{13} - 2\Gamma_{23})(2\Gamma_{12} - \Gamma_{13} - \Gamma_{23}))(\Gamma_{12} - 2\Gamma_{13} + \Gamma_{23}) + 9\mathcal{B}_-(-3\mathcal{C}_-\mathcal{D}_- + \mathcal{B}_+(-2\Gamma_{12} + \Gamma_{13} + \Gamma_{23})))$ and $b = -4\Gamma^2 + 12(\mathcal{B}_+\mathcal{B}_- + \mathcal{C}_+\mathcal{C}_- + \mathcal{D}_+\mathcal{D}_- + \Gamma_{13}\Gamma_{23} + \Gamma_{12}(\Gamma_{13} + \Gamma_{23}))$.

In terms of the diagonal elements, i.e., λ_0 and λ_\pm , the solution of Poincaré equation (22) can be written as

$$\begin{pmatrix} u(t) \\ v(t) \\ w(t) \end{pmatrix} = \sum_{i=0,\pm} d_i e^{\lambda_i t} \begin{pmatrix} 4\mathcal{C}_+\mathcal{C}_- + \Lambda_i \Xi_i \\ 4\mathcal{C}_-\mathcal{D}_- + 2\mathcal{B}_+\Lambda_i \\ 4\mathcal{B}_+\mathcal{C}_+ - 2\mathcal{D}_-\Xi_i \end{pmatrix}, \quad (25)$$

where $\Lambda_i = \lambda_i + 2\Gamma_{12}$ and $\Xi_i = \lambda_i + 2\Gamma_{13}$. The time-independent constants $d_i(\lambda_0, \lambda_+, \lambda_-)$ are determined by the initial conditions, i.e., $u(0) = \sin(2\theta) \cos \phi$, $v(0) = \sin(2\theta) \sin \phi$ and $w(0) = \cos(2\theta)$ from the initial density $\rho_e(0)$.

We find that $d_0(\lambda_0, \lambda_+, \lambda_-) = (4u(0)\mathcal{B}_+^2\mathcal{C}_+ + v(0)\mathcal{D}_-\Xi_2\Xi_3 + \mathcal{B}_+(4u(0)\mathcal{D}_-(\Gamma_{12} - \Gamma_{13}) + w(0)\Lambda_2\Lambda_3 - 2v(0)\mathcal{C}_+(\Lambda_2 + \Xi_3)) + 2\mathcal{C}_-(4u(0)\mathcal{D}_-^2 - 2w(0)\mathcal{B}_+\mathcal{C}_+ + \mathcal{D}_-(-2v(0)\mathcal{C}_+ + w(0)((\Lambda_2 + \Xi_3))))/(4(\mathcal{C}_-\mathcal{D}_-^2 + \mathcal{B}_+(\mathcal{B}_+\mathcal{C}_+ + \mathcal{D}_-(\Gamma_{12} - \Gamma_{13}))) (\lambda_0 -$

$\lambda_+)(\lambda_0 - \lambda_-)$, $d_+(\lambda_0, \lambda_+, \lambda_-) = d_0(\lambda_+, \lambda_-, \lambda_0)$ and $d_-(\lambda_0, \lambda_+, \lambda_-) = d_0(\lambda_-, \lambda_0, \lambda_+)$. The complex numbers λ_{\pm} are very helpful to investigate the neutrino propagation as shown in Ref.[2].

The radius of Poincaré sphere is defined by

$$r^2(t) = \vec{n}(t) \cdot \vec{n}(t) = u^2(t) + v^2(t) + w^2(t), \quad (26)$$

which is a geometric physical quantity with the effects of reflection form $u(t) = \rho_{12}(t) + \rho_{21}(t)$, absorption from $v(t) = i(\rho_{12}(t) - \rho_{21}(t))$ and transition $w(t) = \rho_{11}(t) - \rho_{22}(t)$ between the neutrinos ν_e and ν_{μ} in process of the neutrino mixing and oscillations. Such a radius carries with almost messages of the neutrino mixing and oscillations and therefore provides an important clue to investigate the CPT violating effect in the neutrino mixing and oscillations.

Two azimuthal angles can be defined as

$$\alpha(t) = \cos^{-1} \frac{w(t)}{r(t)}, \beta(t) = \tan^{-1} \frac{v(t)}{u(t)}. \quad (27)$$

In the Poincaré sphere representation, thus, the Poincaré vector is parameterized as

$$\vec{n}(t) = (r(t) \sin \alpha(t) \cos \beta(t), r(t) \sin \alpha(t) \sin \beta(t), r(t) \cos \alpha(t)), \quad (28)$$

and density matrix $\rho(t)$ can be expressed by

$$\rho(t) = \frac{1}{2}(1 + \vec{n}(t) \cdot \vec{\sigma}), \quad (29)$$

with two eigenstates,

$$|\nu_e(t)\rangle = \begin{pmatrix} \cos \frac{\alpha(t)}{2} \\ e^{i\beta(t)} \sin \frac{\alpha(t)}{2} \end{pmatrix}, |\nu_{\mu}(t)\rangle = \begin{pmatrix} \sin \frac{\alpha(t)}{2} \\ -e^{i\beta(t)} \cos \frac{\alpha(t)}{2} \end{pmatrix}, \quad (30)$$

and the corresponding eigenvalues $\lambda_e(t) = \frac{1}{2}(1 + r(t))$ and $\lambda_{\mu}(t) = \frac{1}{2}(1 - r(t))$, respectively. It is obvious that the time-dependent state vectors, $|\nu_e(t)\rangle$ and $|\nu_{\mu}(t)\rangle$, are evolving states of $|\nu_e(0)\rangle$ and $|\nu_{\mu}(0)\rangle$, respectively. In the structure of Poincaré sphere, the two-flavor neutrino state vectors are two orthogonal antipodal points that lie on the azimuthal angles $\alpha(t)$ and $\beta(t)$ of the Poincaré sphere. Thus the evolution of neutrino system is fully mapped onto the Poincaré sphere, where the geometric quantities, i.e., $r(t)$, $\alpha(t)$ and $\beta(t)$, represent the motion trajectory of the two-flavor neutrino mixing and oscillations.

V. TWO-FLAVOR NEUTRINO MIXING AND CPT-VIOLATING MECHANISM

Since the eigenvectors of hermitian operator construct a complete Hilbert subspace, the density matrix $\rho(t)$ can be rewritten as

$$\rho(t) = \frac{1}{2}(1 + r(t)) |\nu_e(t)\rangle\langle\nu_e(t)| + \frac{1}{2}(1 - r(t)) |\nu_{\mu}(t)\rangle\langle\nu_{\mu}(t)|, \quad (31)$$

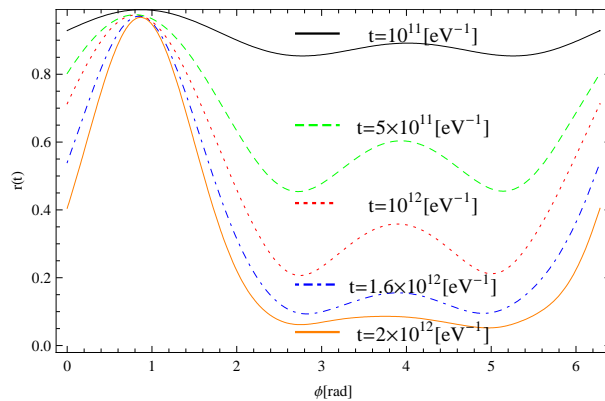


FIG. 1: Radius of Poincaré sphere as a function of ϕ at different evolving times with the parameters $E=10$ MeV, $\Delta m_{21}^2 = 8.0 \times 10^{-5} eV^2$, $c_{11} = 0.095V_0$, $c_{22} = c_{33} = 0.15V_0$, $\theta = 0.188\pi$ and $c_{ij} = (c_{ii}c_{jj})^{1/2}$, where $V_0 = \Delta m_{21}^2/2E$, i.e., the matter potential is equal to the neutrino oscillating frequency in vacuum.

which indicates that two-flavor neutrino mixed states take $(1 \pm r(t))/2$ as the classical mixture probabilities in terms of the radius of Poincaré sphere.

The transition probability of neutrinos can be obtained in terms of such a Poincaré sphere, i.e.,

$$\begin{aligned} P(t) &= \text{Tr} \rho(t) \rho_e(0) \\ &= \frac{1}{2}(1 + r(t)) |\langle \nu_e(0) | \nu_e(t) \rangle|^2 + \frac{1}{2}(1 - r(t)) |\langle \nu_e(0) | \nu_\mu(t) \rangle|^2. \end{aligned} \quad (32)$$

Inserting Eqs. (17) and (30) into Eq. (32), we find

$$P(t) = \frac{1}{2} + \frac{1}{2} r(t) (\cos 2\theta \cos \alpha(t) + \sin 2\theta \sin \alpha(t) \cos(\beta(t) - \phi)), \quad (33)$$

which constructs a connection between the geometric quantity (i.e., radius of Poincaré sphere) and physical observable (i.e., transition probability). Differently from Eq. (14) in the Schrödinger picture, the CP-violating phase ϕ is exactly emerged in the transition probability (33) and the radius of Poincaré sphere (26). Therefore, it is interesting to observe the dynamic behaviors of the radius of Poincaré sphere in terms of the time and CP-violating phase ϕ .

At the initial time $t = 0$, $r(t = 0) = 1$ leads to $\rho(t = 0) = \rho_e(0)$, which includes only a singlet flavor neutrino state. In this case, the neutrino system is in the pure ν_e state that can be represented by the surface points on the Poincaré sphere. For an involving state at the time $t > 0$, $r(t) < 1$ indicates that the density matrix (31) includes two-flavor neutrino states with the classical mixture probabilities $0 < (1 \pm r(t))/2 < 1$ and therefore the neutrino system is in a mixed state with both the two-flavor neutrinos ν_e and ν_μ . It is obvious that such two-flavor neutrino mixed states are corresponding to the interior points of Poincaré sphere. When $r(t) = 0$, the two-neutrino system is in a maximally mixed state, where the neutrino ν_e has the same probability $(1 \pm r(t))/2 = 1/2$ as the neutrino ν_μ .

The radius $r(t)$ illustrates the dynamic characteristics in processing of neutrino mixing and oscillations and defines

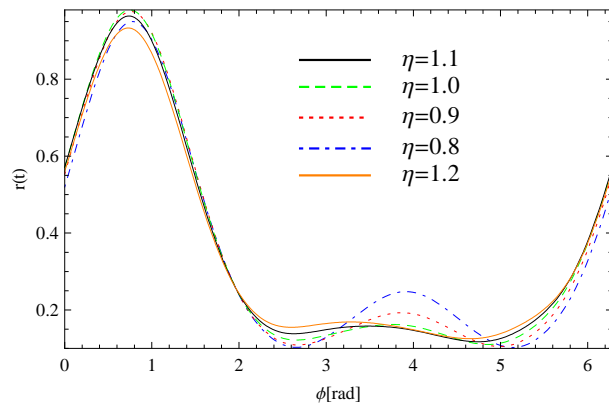


FIG. 2: Radius of Poincaré sphere as a function of ϕ for different matter potentials describing by the proportional rate constant $\eta = V_0/(\Delta m_{21}^2/2E)$ between the matter potential V_0 and neutrino oscillating frequency $\omega = \Delta m_{21}^2/2E$ in vacuum at an evolving time $t = 1.9 \times 10^{12} eV^{-1}$ with the parameters $E = 10$ MeV, $\Delta m_{21}^2 = 8.0 \times 10^{-5} eV^2$, $\theta = 0.188\pi$, $c_{11} = c_{22} = c_{33} = 0.1V_0$ and $c_{ij} = (c_{ii}c_{jj})^{1/2}$.

neutrino mixing degree of freedom in the neutrino oscillations. It is interesting to show the radius $r(t)$ as a function of time and matter potential in order to know the intrinsically inner evolutions of neutrino propagation. The Poincaré radius as a function of CP-violating angle ϕ is shown in Fig. 1 for $V_0 = \Delta m_{21}^2/2E$, i.e., the matter potential V_0 is equal to the neutrino oscillating frequency $\omega = m_{21}^2/2E$ in vacuum, at different times and in Fig. 2 for different proportional rate $\eta = V_0/\omega$ between the matter potential and neutrino oscillating frequency in vacuum for a given time $t = 1.9 \times 10^{12} eV^{-1}$. Interestingly, we see that beside decreasing with increasing time because of interaction with the dissipative reservoir, $r(t)$ oscillates in terms of different amplitudes with an increasing ϕ , where a big wave peak is emerged in the region of $\phi \in [0, \pi/2]$. In the region of $\phi \in [\pi/2, 2\pi]$, a similar phenomenon of spontaneous symmetry breaking is occurred in the two-flavour neutrino mixing and oscillations, where the "Mexican hat" peak is emerged in the radius of Poincaré sphere for the different evolving time (See Fig. 1) and the different matter potential (See Fig. 2).

Generally, spontaneous symmetry breaking is identified with the existence of a non-symmetric lowest energy configuration or state, which accompanies with the dramatic loss of symmetry. The spontaneous symmetry breaking of gauge symmetries is an important component in understanding the origin of particle masses in the standard model of particle physics and the superconductivity of metals. In dynamical gauge symmetry breaking that is a special form of spontaneous symmetry breaking, especially, the bound states of the system itself provide the unstable fields that render the phase transition. Therefore, most phases of matter can be understood through the lens of spontaneous symmetry breaking.

When $t \leq 10^{-11} eV^{-1}$ and $t \geq 2^{-12} eV^{-1}$ as well as $\eta = V_0/(\Delta m_{21}^2/2E) > 1$, the smaller oscillation almost vanishes in the region $\pi/2 \leq \phi \leq \pi$ (See Figs. 1 and 2). The physical reason may be caused by the Majorana-Dirac confusion theorem [3] because the neutrino masses are not important factor for the neutrino oscillations in these cases. Such an

oscillating behavior of Poincaré radius demonstrates that the CP violation enhances the neutrino oscillations just like the matter potential. Therefore, the Poincaré radius $r(t)$ of neutrino oscillations may reveal a dynamic mechanism of CPT violation.

VI. GEOMETRIC PHASE

In situation of pure states, cyclic quantum projections lead to geometric phase which can be understood in terms of geodesic arc on the surface of Poincaré sphere [30]. It is known that the pure and mixed states can be represented in the Poincaré sphere by a unified way, where the pure states correspond to the surface points on the Poincaré sphere and the mixed states are the inside points in the Poincaré sphere. Therefore, we try to extend the geometric phase to the mixed state in terms of the Poincaré sphere structure.

In order to obtain the geometric phase of mixed state, we firstly replace the state vector [31] by the density matrix and then subdivide the smooth curve $\mathcal{C} = \{\rho(t)\}$ into N parts at the points of subdivision $t_0 = 0, t_1, \dots, t_N = t$, where each trajectory is represented by a discrete sequence of associated states $\{\rho_0, \rho_1, \dots, \rho_N, \rho_{N+1} = \rho_0\}$.

Now let us get the Pancharatnam phase in terms of the density matrix, which is defined as

$$\gamma_P = -\arg \text{Tr} \lim_{N \rightarrow \infty} \rho_0(t_0) \rho_1(t_1) \rho_2(t_2) \cdots \rho_{N-1}(t_{N-1}) \rho_N(t_N). \quad (34)$$

Under the one order approximation,

$$\begin{aligned} \langle \sqrt{\lambda_{k_i}} \nu_{k_i}(t_i) | \sqrt{\lambda_{k_{i+1}}(t_{i+1})} \nu_{k_{i+1}}(t_{i+1}) \rangle &\approx \langle \sqrt{\lambda_{k_i}} \nu_{k_i}(t_i) | \sqrt{\lambda_{k_{i+1}}(t_i)} \nu_{k_{i+1}}(t_i) \rangle \\ &+ \langle \sqrt{\lambda_{k_i}} \nu_{k_i}(t_i) | \frac{d}{dt_i} | \sqrt{\lambda_{k_{i+1}}(t_i)} \nu_{k_{i+1}}(t_i) \rangle \Delta t_i, \end{aligned} \quad (35)$$

where $\Delta t_i = t_{i+1} - t_i$, we have

$$\begin{aligned} \rho_i(t_i) \rho_{i+1}(t_{i+1}) &\approx \sum_{k_i, k_{i+1}} | \sqrt{\lambda_{k_i}(t_i)} \nu_{k_i}(t_i) \rangle \langle \sqrt{\lambda_{k_{i+1}}(t_{i+1})} \nu_{k_{i+1}}(t_{i+1}) | \\ &\times \left(\langle \sqrt{\lambda_{k_i}(t_i)} \nu_{k_i}(t_i) | \sqrt{\lambda_{k_{i+1}}(t_i)} \nu_{k_{i+1}}(t_i) \rangle + \langle \sqrt{\lambda_{k_i}} \nu_{k_i}(t_i) | \frac{d}{dt_i} | \sqrt{\lambda_{k_{i+1}}(t_i)} \nu_{k_{i+1}}(t_i) \rangle \Delta t_i \right) \end{aligned} \quad (36)$$

Inserting Eq. (36) into Eq. (34), the Pancharatnam phase can be expressed as

$$\begin{aligned} \gamma_P &= -\arg \text{Tr} \lim_{N \rightarrow \infty} \sum_{k_0, k_1, \dots, k_N} | \sqrt{\lambda_{k_0}} \nu_{k_0}(t_0) \rangle \langle \sqrt{\lambda_{k_N}} \nu_{k_N}(t_N) | \\ &\times \prod_{i=0}^N \left(\langle \sqrt{\lambda_{k_i}(t_i)} \nu_{k_i}(t_i) | \sqrt{\lambda_{k_{i+1}}(t_i)} \nu_{k_{i+1}}(t_i) \rangle + \langle \sqrt{\lambda_{k_i}} \nu_{k_i}(t_i) | \frac{d}{dt_i} | \sqrt{\lambda_{k_{i+1}}(t_i)} \nu_{k_{i+1}}(t_i) \rangle \Delta t_i \right). \end{aligned} \quad (37)$$

In terms of the adiabatic approximation, we drop off the nondiagonal terms. We find

$$\begin{aligned}
\gamma_P &\approx -\arg \lim_{N \rightarrow \infty} \langle \sqrt{\lambda_e(t_N)} \nu_e(t_N) | \sqrt{\lambda_e(t_0)} \nu_e(t_0) \rangle \prod_{i=0}^N \left(\lambda_e(t_i) + \langle \sqrt{\lambda_e(t_i)} \nu_e(t_i) | \frac{d}{dt_i} | \sqrt{\lambda_e(t_i)} \nu_e(t_i) \rangle \Delta t_i \right) \\
&\quad - \arg \lim_{N \rightarrow \infty} \langle \sqrt{\lambda_\mu(t_N)} \nu_e(t_N) | \sqrt{\lambda_\mu(t_0)} \nu_e(t_0) \rangle \prod_{i=0}^N \left(\lambda_\mu(t_i) + \langle \sqrt{\lambda_\mu(t_i)} \nu_\mu(t_i) | \frac{d}{dt_i} | \sqrt{\lambda_\mu(t_i)} \nu_\mu(t_i) \rangle \Delta t_i \right) \\
&\approx -\arg \lim_{N \rightarrow \infty} \langle \sqrt{\lambda_e(t_N)} \nu_e(t_N) | \sqrt{\lambda_e(t_0)} \nu_e(t_0) \rangle \exp \sum_{i=0}^N \left(-\lambda_\mu(t_i) + \langle \sqrt{\lambda_e(t_i)} \nu_e(t_i) | \frac{d}{dt_i} | \sqrt{\lambda_e(t_i)} \nu_e(t_i) \rangle \Delta t_i \right) \\
&\quad - \arg \lim_{N \rightarrow \infty} \langle \sqrt{\lambda_\mu(t_N)} \nu_e(t_N) | \sqrt{\lambda_\mu(t_0)} \nu_e(t_0) \rangle \exp \sum_{i=0}^N \left(-\lambda_e(t_i) + \langle \sqrt{\lambda_\mu(t_i)} \nu_\mu(t_i) | \frac{d}{dt_i} | \sqrt{\lambda_\mu(t_i)} \nu_\mu(t_i) \rangle \Delta t_i \right) \\
&= \arg \sum_{i=e,\mu} \left(\sqrt{\lambda_i(0) \lambda_i(t)} \langle \nu_i(0) | \nu_i(t) \rangle \right) - \Im \sum_{i=e,\mu} \int_0^t \lambda_i(t) \langle \nu_i(t) | \frac{d}{dt} | \nu_i(t) \rangle dt, \tag{38}
\end{aligned}$$

where is invariant under the $U(1)$ gauge transformation,

$$| \nu_i(t) \rangle \rightarrow | \nu'_i(t) \rangle = e^{i\varphi(t)} | \nu_i(t) \rangle, (i = e, \mu), \tag{39}$$

with the arbitrary phase factors $\varphi(t)$. For the two-level system, the Pacaré sphere, together with an overall $U(1)$ phase, provides a complete $SU(2)$ description [32, 33].

In comparison with the density operator (31) with a $U(1) \times U(1)$ invariant, we see that Eq. (38) includes the contributions of two states and their distribution probabilities in the density matrix but keeps only the $U(1)$ invariant similar to the gauge fixing [34, 35], i.e., $\varphi_e(t) = \varphi_\mu(t) = \varphi(t)$. The geometric phase under the gauge fixing [36] was verified for an incoherent average of pure state interference in terms of the nuclear magnetic resonance technique [37].

In Eq. (38), the first term on the right hand provides a message of phase differences between the initial and final eigenstates of density matrix and therefore is called as a total phase. At the initial time $r(t=0) = 1$, the two classical mixed probabilities $\lambda_\mu(0) = (1 - r(0))/2 = 0$ and $\lambda_e(0) = (1 + r(0))/2 = 1 \neq 0$. Thus the evolving state of flavor neutrino ν_μ does not contribute to such a total phase. The total phase can be expressed in terms of the Poincaré parameters, i.e.,

$$\gamma_t = \tan^{-1} \frac{\sin(\beta(t) - \beta(0)) \sin \frac{\alpha(0)}{2} \sin \frac{\alpha(t)}{2}}{\cos \frac{\alpha(0)}{2} \cos \frac{\alpha(t)}{2} + \cos(\beta(t) - \beta(0)) \sin \frac{\alpha(0)}{2} \sin \frac{\alpha(t)}{2}}. \tag{40}$$

The second term depends on the dynamic evolution of eigenstates of density matrix and therefore is called as dynamic phase and can be separated into two parts. The dynamic phase γ_{d1} from the neutrino ν_e is given by

$$\gamma_{d1} = -\frac{1}{2} \int_0^t (1 + r(t)) \sin^2 \frac{\alpha(t)}{2} d\beta(t), \tag{41}$$

and γ_{d2} from the neutrino ν_μ is

$$\gamma_{d2} = -\frac{1}{2} \int_0^t (1 - r(t)) \cos^2 \frac{\alpha(t)}{2} d\beta(t). \tag{42}$$

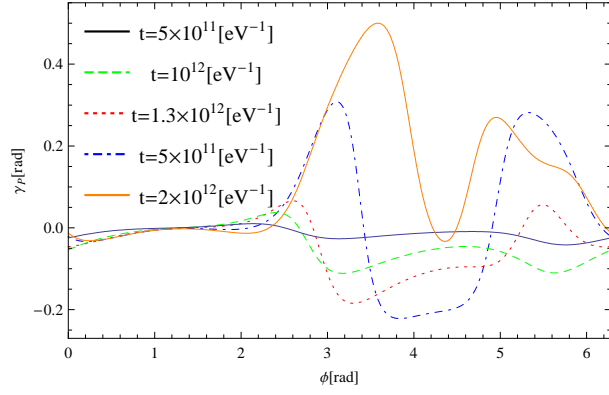


FIG. 3: Pancharatnam phase as a function of ϕ at different evolving times with the parameters $E=10$ MeV, $\Delta m_{21}^2 = 8.0 \times 10^{-5} eV^2$, $\theta = 0.188\pi$, $c_{11} = 0.095V_0$, $c_{22} = c_{33} = 0.15V_0$, $c_{ij} = (c_{ii}c_{jj})^{1/2}$ and $\eta = 1$.

It is known that the dynamic phase of pure state can be extracted quite easily in Hamiltonian formulation. Generally, a mixed state is expressed in many different expansions as a classical probabilistic mixture of pure states. Therefore, it is necessary to consider the classical probability distributions (i.e., the eigenvalues of density matrix) in case of mixed state. Under the transformation,

$$|\tilde{\nu}_i(t)\rangle = |\sqrt{\lambda_i(t)}\nu_i(t)\rangle \exp\left(-\int_0^t \lambda_i(t)\langle\nu_i(t)|\frac{d}{dt}|\nu_i(t)\rangle dt\right), (i = e, \mu), \quad (43)$$

the Pancharatnam phase (38) can be reexpressed as

$$\gamma_P = \arg \sum_{i=e,\mu} \langle\tilde{\nu}_i(0)|\tilde{\nu}_i(t)\rangle, \quad (44)$$

which extracts the dynamic phases of mixed state.

VII. DISCUSSIONS

The Pancharatnam phases as a function of CP-violating angle ϕ are shown in Figs. 3-5 at different evolving times under the fluctuational fields. We find that the Pancharatnam phases are an oscillating function of ϕ and related to the evolving time. The different curve shapes of Pancharatnam phases show that the time reversal is not invariant, in turn, the CPT symmetry is violated. The results provide a useful tool to measure the neutrino property in the experiments in terms of the time-dependent geometric phase.

From Fig. 3, we see that the Pancharatnam phases are small negative values in the region of $0 \leq \phi \leq 4\pi/5$ and show almost the same behavior for different evolving times. In the other regions, however, the oscillations of Pancharatnam phases are different and dependent on the evolving times. These different behaviors are resulted from the mixing effects of both the flavor neutrinos ν_e and ν_μ . The contributions of the neutrinos ν_e and ν_μ to the Pancharatnam phases are shown in Fig. 4. We find that the evolving ways of the dynamic phase γ_{d1} of the neutrino ν_e are different

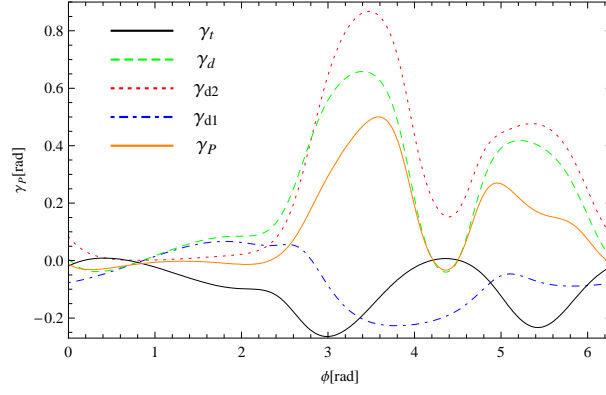


FIG. 4: Various different phases in the neutrino mixing and oscillations as a function of ϕ at an evolving time $t = 2 \times 10^{12} eV^{-1}$ with the parameters $E = 10$ MeV, $\Delta m_{21}^2 = 8.0 \times 10^{-5} eV^2$, $\theta = 0.188\pi$, $c_{11} = 0.095V_0$, $c_{22} = c_{33} = 0.15V_0$, $c_{ij} = (c_{ii}c_{jj})^{1/2}$ and $\eta = 1$, where γ_{d1} and γ_{d2} are dynamic phases of the neutrinos ν_e and ν_μ , respectively. $\gamma_d = \gamma_{d1} + \gamma_{d2}$ is a total dynamic phase, γ_t is a total phase and γ_P is a Pancharatnam phase.

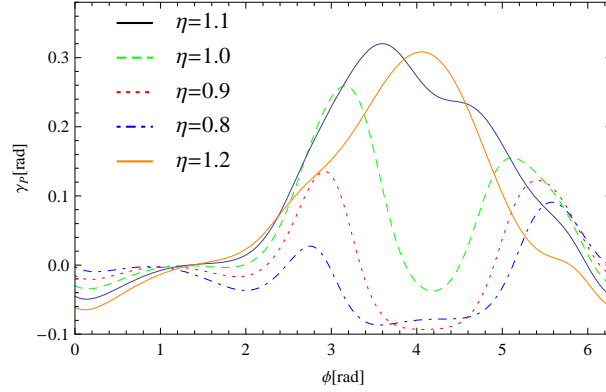


FIG. 5: Pancharatnam phase as a function of ϕ for different matter potentials at an evolving time $t = 1.9 \times 10^{12} eV^{-1}$ with the parameters $E = 10$ MeV, $\Delta m_{21}^2 = 8.0 \times 10^{-5} eV^2$, $\theta = 0.188\pi$, $c_{11} = c_{22} = c_{33} = 0.1V_0$ and $c_{ij} = (c_{ii}c_{jj})^{1/2}$.

from γ_{d2} of the neutrino ν_μ , where γ_{d1} is a two-peak structure in the region of $\phi \in [4\pi/5, 2\pi]$ differently from the wave trough of γ_{d2} and the iterating results of both γ_{d1} and γ_{d2} lead to the total dynamic phase $\gamma_d = \gamma_{d1} + \gamma_{d2}$. Therefore, the mixing effects of neutrinos are very important to the geometric phase because the neutrino system is in a superposition with the ν_e and ν_μ . Our results are different from Ref. [20], where the kinematic approach was used and the mixture probabilities were taken as the constants $\sqrt{\lambda_k(t=0)\lambda_k(t=T)}$ (T is a quasicyclity, $k = e, \mu$). We know that $\lambda_\mu(t=0) = (1 - r(t=0))/2 = 0$ and therefore the contribution of the neutrino ν_μ to the geometric phase vanishes in all evolving processes. Thus the kinematic approach to geometric phase does not include the mixing effect.

The Pancharatnam phases of neutrino oscillations depend also on the matter potential as shown in Fig. 5. When the matter potential V_0 is larger than the neutrino oscillating frequency $\omega = \Delta m_{21}^2/(2E)$ in vacuum, i.e., $\eta > 1$, the two peaks structures ($\eta < 1$) become single peak.

VIII. DETECTIONS

It is well-known that the conventional way to address the Majorana issue given the small mass scale of the neutrino in this field is neutrinoless double beta decay (NDBD). Because of the extremely low efficiency of direct neutrino measurements in terms of the physical observable (i.e., transition probability of neutrino), unfortunately, it is necessary to accomplish exquisitely complex state-of-the-art rare event infrastructure.

Another observable is geometric phase in the neutrino mixing and oscillations. Thus the time-dependent Pancharatnam phase can be helpful in the detection of CPT-violation due to an enhanced flexibility in the choice of evolutions as shown in Figs. 3-5. This phase factor can be realized by the neutrino split-beam-interference experiment [10]. Unfortunately, the spatially beam splitting experiment is almost impossible for a tiny interaction cross section. When the neutrino propagates through dissipative matter, on the other hand, the environment is usually unknown. Thus it is difficult to determine the decay coefficients c_{ij} in the neutrino experiments.

A possible alternative approach is quantum simulation, where the simulation of fundamental particle physics properties using a controllable quantum system is an increasing and interesting topic in both particle physics and condense matter physics [37–41]. Thus we propose to detect the Pancharatnam phase by simulating the environment of neutrino propagation in terms of a controllable physical field (e.g., magnetic field), $\mathcal{M}_0 = \frac{1}{2}V_0\sigma_z$, with corresponding fluctuation fields $\mathcal{M}_i = d_i\sigma_i$ (e.g., fluctuational magnetic fields), and a nuclear-magnetic-resonance (NMR) system with the Hamiltonian [42],

$$\mathcal{H}_{NMR} = -\frac{1}{2}\omega \cos 2\theta \sigma_z + \frac{1}{2}\omega \sin 2\theta \cos \phi \sigma_x + \frac{1}{2}\omega \sin 2\theta \sin \phi \sigma_y, \quad (45)$$

which has the same form as Eq. (1) beside the firm term for the two-flavor neutrino oscillations in medium and the simulating parameters are taken in terms of the parameters from the neutrino oscillations, i.e., $\omega = \Delta m_{21}^2/2E \in [4.0 \times 10^{-12}, 4.0 \times 10^{-11}]eV^{-1}$, $V_0 = \eta \Delta m_{21}^2/2E \in [4\eta \times 10^{-12}, 4\eta \times 10^{-11}]eV^{-1}$ and $d_i = 0.1V_0 \in [4\eta \times 10^{-13}, 4\eta \times 10^{-12}]eV^{-1}$ for the neutrino square-mass difference $\Delta m_{12}^2 = 8.0 \times 10^{-5}eV^2$ and energy range $E \in [1, 10]MeV$ with a controlling and adjusting constant η as shown in Figs. 1-5. Thus the Hamiltonian (1) of neutrino oscillations is converted equivalently into $\mathcal{H} = \mathcal{M}_0 + \mathcal{H}_{NMR}$, where the constant term \mathcal{H}_0 in Eq. (1) is dropped off because it only contributes an overall phase factor. Next, using the relation $[\sigma_i\rho, \sigma_j] + [\sigma_i, \rho\sigma_j] = -[\sigma_i, [\sigma_j, \rho]]$, the dissipative terms (16) in the master equation (15) can be reexpressed by

$$\mathcal{L}\rho = -\frac{1}{2} \sum_{i,j=x,y,z} [\mathcal{M}_i, [\mathcal{M}_j, \rho]], \quad (46)$$

where the double commutator results in a time-irreversibility and is helpful to study the CPT violation. Thus the environment effects can also simulated by the controlable fluctuational fields. Comparing Eq. (46) with Eq. (16), we take $c_{ij} = d_i d_j$ as the decay coefficients.

In terms of Eqs. (45)-(46), we construct a connection between the neutrino oscillation and NMR experiment. It was demonstrated in the NMR experiment that an open system can be simulated by varying the choice of mapping between the simulated system and the simulator [37]. An important advantage of quantum simulations [38–41] is that the values of the neutrino mass square difference, mixing angle of vacuum, propagating energy, CP-violating angle and dissipative coefficients can be measured just by controlling the fluctuational field and NMR parameters. On the other hand, it becomes possible and easy to detect the Pancharatnam phase of neutrino through dissipative matter in terms of the controllable quantum system, i.e., NMR system.

IX. CONCLUSIONS

In summary, the neutrino mixing and oscillations are modeled on the basis of a two-dimensional Hilbert space with an intrinsic CP-violating phase under the dissipative matter. The geometric representation is given by mapping the dynamic master equation onto the Poincaré sphere structure. We show that the mixture of two-flavor neutrino system is in terms of the Poincaré radius depending on the intrinsic CP-violating phase. We find that, especially, the phenomena of both similar spontaneous symmetry breaking mechanism and Majorana-Dirac neutrino confusion are emerged in such a time-dependent Poincaré radius from the neutrino mixing and oscillations. Moreover, we find that the CPT-violating effect is enhanced in the time-dependent geometric phase under the neutrino propagating process. The results provide a new way to test the Dirac vs Majorana neutrinos and Majorana-Dirac confusion theorem as well as observe the CPT-violation. At last, we propose to detect such a geometric phase in terms of the quantum simulation by using a controllable physical field and NMR system.

Acknowledgments

This work is supported by the Natural Science Foundation of China under Grant No. 11565015 and No.11365012, the Natural Science Foundation of Jiangxi Province, China under Grant No. 20132BAB202008, the Foundation of Science and Technology of Education Office of Jiangxi Province under No. GJJ13235.

Hui Pan thanks the supports of the Science and Technology Development Fund from Macao SAR (FDCT-068/2014/A2 and FDCT-132/2014/A3), and Multi-Year Research Grants (MYRG2014-00159-FST and MYRG2015-0015-FST) and Start-up Research Grant (SRG- 2013-00033-FST) from Research and Development Office at University of Macau.

[1] C. Giunti and C. W. Kim, *Fundamentals of Neutrino Physics and Astrophysics* (Oxford University Press, 2007).
 [2] B. Kayser, *Neutrino Oscillation Physics*, arXiv:1206.4325v2.

- [3] Abhish Dev, P. Ramadevi and S. Uma Sankar, Non-zero θ_{13} and δ_{CP} in a neutrino mass model with A_4 symmetry, JHEP **11** (2015) 034.
- [4] B. Kayser, Majorana neutrinos and their electromagnetic properties, Phys. Rev. D **26** (1982)1662.
- [5] S. M. Bilenky and S. T. Petcov, Massive neutrinos and neutrino oscillations, Rev. Mod. Phys. **59** (1987) 671.
- [6] K. Abe et al, Observation of Electron Neutrino Appearance in a Muon Neutrino Beam, Phys. Rev. Lett. **112** (2014) 061802.
- [7] F. P. An et al, Observation of Electron-Antineutrino Disappearance at Daya Bay, Phys. Rev. Lett. **108** (2012) 171803.
- [8] J. K. Ahn, et al. Observation of Reactor Electron Antineutrinos Disappearance in the RENO Experiment. Phys. Rev. Lett. **108** (2012) 191802.
- [9] F. P. An et al, Independent measurement of the neutrino mixing angle θ_{13} via neutron capture on hydrogen at Daya Bay, Phys. Rev. D **90** (2014) 071101.
- [10] T. D. Gutierrez, Observation of Reactor Electron Antineutrinos Disappearance in the RENO Experiment, Phys. Rev. Lett. **96** (2006) 121802.
- [11] P. Mehta, Topological phase in two flavor neutrino oscillations, Phys. Rev. D **79** (2009) 096013.
- [12] J.-C. Peng, Neutron electric dipole moment experiments, Mod. Phys. Lett. A **23** (2008) 1397.
- [13] C.-H. Chen, et al, Investigation of $B(u, \alpha) \rightarrow (\pi, \kappa)\pi$ decays within unparticle physics, Phys. Lett. B **671** (2009) 250.
- [14] B. Pontecorvo, Neutrino Experiments and the Problem of Conservation of Leptonic Charge, Sov. Phys. JETP **26** (1968) 984.
- [15] Sanjib Kumar Agarwalla, Yee Kao, Tatsu Takeuchi, Analytical Approximation of the Neutrino Oscillation Matter Effects at large θ_{13} , JHEP **04** (2014) 047.
- [16] Emilio Ciuffoli, Jarah Evslin, Xinmin Zhang, The Leptonic CP Phase from Muon Decay at Rest with Two Detectors, JHEP **1412** (2014) 051.
- [17] Y. Pehlivan et al, Neutrino Magnetic Moment, CP Violation and Flavor Oscillations in Matter, Phys. Rev. D **90** (2014) 065011.
- [18] T. K. Kuo and J. Pantaleone, Neutrino oscillations in matter, Rev. Mod. Phys. **61** (1989) 937.
- [19] A. Capolupo, Probing CPT violation in meson mixing by non-cyclic phase, Phys. Rev. D **84** (2011) 116002.
- [20] J. Dajka, J. Syska, J. Luczka, Geometric phase of neutrino propagating through dissipative matter, Phys. Rev. D **83** (2011) 097302.
- [21] F. N. Loreti and A. B. Balantekin, Neutrino oscillations in noisy media, Phys. Rev. D **50**(1994) 4762.
- [22] N. E. Mavromatos and S. Sarkar, Methods of approaching decoherence in the flavour sector due to space-time foam, Phys. Rev. D **74** (2006) 036007.
- [23] Jiawei Hua and Hongwei Yu, Geometric phase outside a Schwarzschild black hole and the Hawking effect, JHEP **09** (2012) 062.
- [24] Zehua Tian and Jiliang Jing, Geometric phase of two-level atoms and thermal nature of de Sitter spacetime, JHEP **04** (2013) 109.
- [25] C. Giunti, No Effect of Majorana phases in neutrino oscillations, Phys. Lett. B **686** (2010) 41.
- [26] G. Lindblad, On the generators of quantum dynamical semigroups, Commun. Math. Phys. **48**(1976) 119.
- [27] C. W. Kim, J. Kim, W. K. Sze, Geometrical representation of neutrino oscillations in vacuum and matter, Phys. Rev. D **37** (1988) 1072.
- [28] John Ellis, Jae Sik Leeb and Apostolos Pilaftsis, A geometric approach to CP violation: applications to the MCPMFV SUSY model, JHEP **10** (2015) 049.
- [29] Z. S. Wang and Q. Liu, Geometric phase and spinorial representation of mixed state, Phys. Lett. A **377** (2013) 3272.
- [30] Joseph Samuel and Rajendra Bhandari, General Setting for Berry's Phase, Phys. Rev. Lett. **60** (1988) 2339.
- [31] N. Mukunda and R. Simon, Quantum Kinematic Approach to the Geometric Phase. I. General Formalism, Ann. Phys. **228**(1993)205.
- [32] D. B. Uskov and A. R. P. Rau, Geometric phase for N-level systems through unitary integration, Phys. Rev. A **74** (2006) 030304(R).
- [33] D. Uskov, A.R.P. Rau, Geometric phases and Bloch-sphere constructions for SU(N) groups with a complete description of the SU(4) group, Phys. Rev. A **78** (2008) 022331.
- [34] E. Sjöqvist, A. K. Pati, A. Ekert, J. S. Anandan, M. Ericsson, D. K. L. Oi and V. Vedral, Phys. Rev. Lett. **85** (2000) 2845.
- [35] E. Sjöqvist, J. Phys. A: Math. Gen. **37** (2004) 7393.
- [36] J. F. Du, P. Zou, M. Shi, L. C. Kwek, J. W. Pan, C. H. Oh, A. Ekert, D. K. L. Oi and M. Ericsson M, Phys. Rev. Lett. **91** (2003) 100403.
- [37] C. H. Tseng et al, Quantum simulations with natural decoherence, Phys. Rev. A **62**(2000) 032309.
- [38] R. Gerritsma et al, Quantum simulation of the Dirac equation, Nature **463** (2010) 68.
- [39] R. Gerritsma, et al., Quantum simulation of the Klein paradox with trapped ions, Phys. Rev. Lett. **106** (2011) 060503.
- [40] Z. S. Wang, X. Cai and H. Pan, Trapped ionic simulation of neutrino electromagnetic properties in neutrino oscillation, Nucl. Phys. B **900** (2015) 560.
- [41] J. Casanova, et al., Quantum simulation of the Majorana equation and unphysical operations, Phys. Rev. X **1** (2011) 021018.
- [42] Z. S. Wang et al., Nonadiabatic geometric quantum computation, Phys. Rev. A **76** (2007) 044303.